

Monitoring Ground-Surface Heating During Expansion of the Casa Diablo Production Well Field at Mammoth Lakes, California

Deborah Bergfeld¹, R. Greg Vaughan², William C. Evans¹, and Eric Olsen³

¹U.S. Geological Survey, Menlo Park, CA

²U.S. Geological Survey, Astrogeology Science Center, Flagstaff, AZ

³Aerial Thermal Imaging, Salt Lake City, UT

Keywords

Thermal Infrared (TIR) imagery, diffuse CO₂ degassing, ground heating, Long Valley caldera, geothermal monitoring

ABSTRACT

The Long Valley hydrothermal system supports geothermal power production from 3 binary plants (Casa Diablo) near the town of Mammoth Lakes, California. Development and growth of thermal ground at sites west of Casa Diablo have created concerns over planned expansion of a new well field and the associated increases in geothermal fluid production. To ensure that all areas of ground heating are identified prior to new geothermal development, we obtained high-resolution aerial thermal infrared imagery across the region. The imagery covers the existing and proposed well fields and part of the town of Mammoth Lakes.

Imagery results from a predawn flight on Oct. 9, 2014 readily identified the Shady Rest thermal area (SRST), one of two large areas of ground heating west of Casa Diablo, as well as other known thermal areas smaller in size. Maximum surface temperatures at 3 thermal areas were 26–28 °C. Numerous small areas with ground temperatures >16 °C were also identified and slated for field investigations in summer 2015. Some thermal anomalies in the town of Mammoth Lakes clearly reflect human activity.

Previously established projects to monitor impacts from geothermal power production include yearly surveys of soil temperatures and diffuse CO₂ emissions at SRST, and less regular surveys to collect samples from fumaroles and gas vents across the region. Soil temperatures at 20 cm depth at SRST are well correlated with diffuse CO₂ flux, and both parameters show little variation during the 2011–14 field surveys. Maximum temperatures were between 55–67 °C and associated CO₂ discharge was around 12–18 tonnes per day. The carbon isotope composition of CO₂ is fairly uniform across the area ranging between –3.7 to –4.4 ‰. The gas composition of the Shady Rest fumarole however has varied with time, and H₂S concentrations in the gas have been increasing since 2009.

Introduction

The Long Valley caldera in eastern California supports a large hydrothermal system that supplies heat and fluids for geothermal power production at the Casa Diablo power plant (Fig. 1). Initial power production began in 1985 from a single 10 MW binary plant that uses isobutane as the working fluid. Two additional 15 MW binary plants came online in 1990 for a combined capacity of 40 MWe (Sorey and others, 1995).

Drilling evidence places the upflow zone for the Long Valley hydrothermal system in the west moat of Long Valley caldera with a maximum temperature of ~220 °C measured in well 44-16 (Sorey and others, 1991). Shallow west-to-east directed lateral outflow is identified from temperature reversals at depth and from cooler temperatures in wells east of 44-16 (Sorey and others, 1991). In the western part of the caldera much of the flow occurs within permeable rhyolite caldera fill deposits (Suemnicht and others, 2007). Fluid temperatures in wells at the power plant are about 170 °C at ~150 m depth, and temperatures decrease to boiling at discharge points along Hot Creek Gorge (Sorey and others,

1991). Several weak steam vents (fumaroles) are found along the flow path at locations both west and east of the power plant (Fig. 1).

The higher temperatures in the west moat provided incentive for construction of the Basalt Canyon pipeline that carries 180 °C fluids from two wells (57-25 and 66-25) located ~3 km west of the power plant (Suemnicht and others, 2007). Proposed changes to the production scheme include increased fluid production from additional wells near the town of Mammoth Lakes. Several additional wells have been drilled or are in planning, but only the 57-25 and 66-25 wells are currently in use.

Fluid production from 57-25 and 66-25 wells began in the summer of 2006 and subsequently, we documented an increase in the size of several pre-existing areas of thermal ground ~500 m north of the wells, as well as formation of a new area of ground heating (Bergfeld and Evans, 2011). The larger areas of ground heating and steam discharge are readily identified by the presence of dead and dying mature pine trees, are commonly associated with the presence of cheat grass, and contain sections of bare ground. Yearly measurements of diffuse CO₂ emissions and shallow soil temperatures are performed across the most active sites to track changes in thermal fluid upflow related to fluid production.

Prior to expanded geothermal development it is desirable to document all existing areas of thermal ground. Although large areas of ground heating are easy to recognize, the presence of several small localized areas of ground heating creates some questions about the completeness of the thermal inventory. Given the size of the hydrothermal system it would be difficult to conduct a thorough survey of the entire area on foot, so we initiated a study to inventory the thermal ground using aerial thermal infrared (TIR) imaging, collected using a fixed-wing aircraft flown before sunrise.

Methods

Thermal Infrared Data Collection

High-resolution airborne TIR data were acquired by the Aerial Thermal Imaging (ATI) LLC of Salt Lake City, Utah, on October 9, 2014 during predawn hours. Data were collected using a custom TIR camera system built by ATI. The camera system uses an uncooled vanadium oxide detector that is sensitive to radiance in the 7–14 micron wavelength range, and collects images as a series of overlapping frames. The raw radiance data are calibrated to surface temperature using an assumed emissivity and an internal blackbody measurement and validated by concurrent ground temperature measurements. The resulting temperature is accurate to ± 0.5 °C. Ground temperatures were collected at 3 background and 3 thermal locations using TREX-8 dataloggers with the temperature probe placed in the top cm of the soil, and these records will be used to make final adjustments to TIR temperatures.

Two groups of images were acquired from a Cessna 210 fixed-wing aircraft flying at altitudes of 730 m (2400 ft) and 1830 m (6000 ft) above ground level, which yielded pixel sizes of 0.9 m (3 ft) and 2.3 m (7.5 ft), respectively (Fig. 1). Data from a camera core integrated WAAS GPS/IMU were acquired simultaneously for pixel geolocation. ATI global contrasting converting software uses histogram methods to stitch image frames into a single image mosaic. Due to uncertainties (of up to 120 m) in the automated pixel geolocation and image georegistration process, temperature map data products were manually adjusted to match known surface features and to accurately locate anomalously warm pixels.

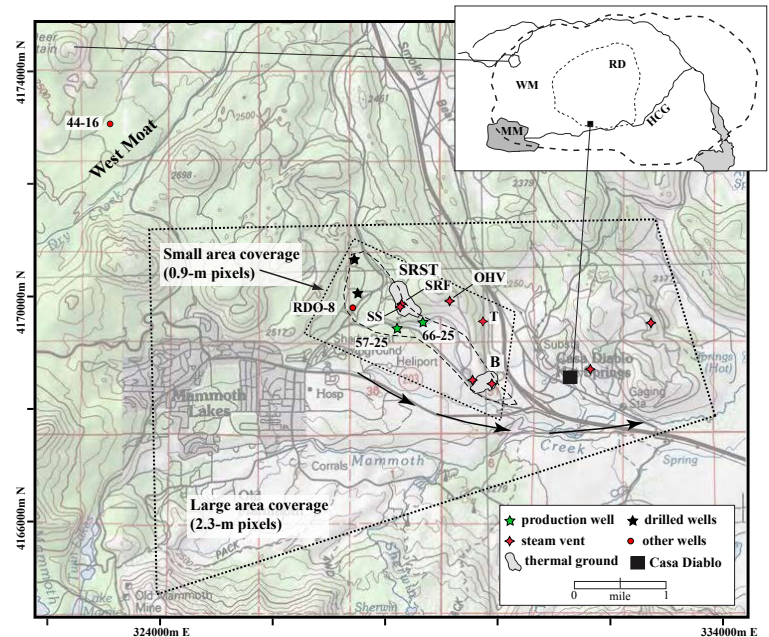


Figure 1. Map showing the location of the Shady Rest thermal area (SRST), the Casa Diablo power plant, and production wells and steam vents discussed in the text. Arrows indicate the general flow direction of the Long Valley hydrothermal system. Thin dashed line is a generalized outline of the proposed expansion of the production well field. Thick dotted lines show the approximate coverages of TIR imagery acquired in October 2014. Heavy dashed line (inset) shows the topographic margin of the Long Valley caldera. HCG = Hot Creek Gorge, RD = Resurgent Dome, SRF = Shady Rest fumarole, SS = steaming stump, T = Teapot gas site, MM = Mammoth Mountain, OHV = Obsidian Hills gas vent, WM = West Moat, B = Basalt Canyon thermal area (Bergfeld and Evans, 2011). Drilled wells (black stars) were not producing at the time of writing.

Diffuse CO₂ Flux Measurements and Associated Ground Temperature

In 2006 we began conducting yearly surveys of diffuse CO₂ emissions and soil temperatures over a grid of measurement points in an existing area of thermal ground (Fig. 1, SRST) (Bergfeld and Evans, 2011). Between 2006 and 2011 the grid coverage increased from 78 sites covering ~61,000 m² to 129 sites covering 100,000 m². The measurement grid includes several sites with steaming ground and a gas vent known as the Shady Rest fumarole (SRF). Diffuse CO₂-flux measurements are made using a West Systems flux meter equipped with a LI-COR® 820 infrared CO₂ analyzer and an accumulation chamber. The soil temperature at 20 cm is measured using a thermocouple and digital thermometer coincident with each flux measurement.

The diffuse flux is reported as grams of CO₂ per square meter per day (g m⁻² d⁻¹). Total discharge is determined by multiplying the mean flux for all the sites by the grid area and is reported in units of metric tonnes of CO₂ emitted per day (t d⁻¹). For this report we use sequential Gaussian simulation (sGs) module within GSLIB (Geostatistical software; Deutsch and Journel, 1998) to estimate the mean flux and the 95-percent upper and lower boundaries on the determined discharge, as outlined in Cardellini and others (2003) and Lewicki and others (2005). Results from the 2006–2010 investigation of SRST and the nearby Basalt Canyon thermal area (“B” in Figure 1) are discussed in full in Bergfeld and Evans (2011).

Gas Collection and Analysis

Gases from vents and steaming ground are collected into evacuated glass bottles. The collection apparatus includes a stainless steel tube, Tygon® tubing, and a hand-held infrared CO₂ analyzer that is placed at the downstream end of the sampling apparatus after the glass bottle. The stainless steel tube is inserted into the main area of gas upflow and a pump in the analyzer is used to draw gas through the system. The CO₂ concentrations are monitored to determine the appropriate depth for sampling. Once determined, the analyzer is shut off and the sample bottle opened.

Gases were analyzed using a PerkinElmer Sigma 3 gas chromatograph with He and Ar carrier gases and a thermal conductivity detector at the U.S. Geological Survey (USGS) in Menlo Park, California. Hydrocarbon concentrations in two samples from 2014 were determined using a Varian 3800 gas chromatograph with He carrier gas and a flame ionization detector. Stable isotope analysis of carbon isotope ratios (δ¹³C) in CO₂ were performed by mass spectrometry at the USGS Stable Isotope Laboratory in Reston, Virginia (Coplen, 1973; Revesz and Coplen, 2006).

Results and Discussion

Aerial Thermal Infrared Findings

We have focused our initial efforts on the TIR data collected over the large area with 2.3-m pixels (Fig. 1). The pre-dawn TIR-derived pixel temperatures for this area range from ~9–28 °C. Areas that are barren of vegetation and fields with short grasses have the lowest temperatures (~9–12 °C). Forested areas range in temperature from ~12–16 °C. Areas with a pixel temperature >16 °C were designated as thermally anomalous and are highlighted red in Figure 2. The selection of the 16 °C threshold was based on a visual assessment of the data and designed to highlight only localized clusters of bright pixels that were likely to be geothermal in origin and to minimize the selection of more widely distributed bright pixels in large forested areas and bright pixels that were artifacts of the image mosaic processing.

The airborne TIR data identified several clusters of bright pixels (interpreted as anomalously warm ground) in the SRST grid and also several clusters of thermal ground east of SRST, including a site known as the Teapot (Fig. 2). The highest pixel temperatures measured at SRST and Teapot were 27 °C and 26 °C, respectively. The highest pixel temperature measured in the entire area (28 °C) was located at a known thermal site, the Obsidian Hill gas vent (OHV), between SRST and Teapot (Fig. 2). Additionally, a small group of bright pixels at the Sierra Star golf course represents

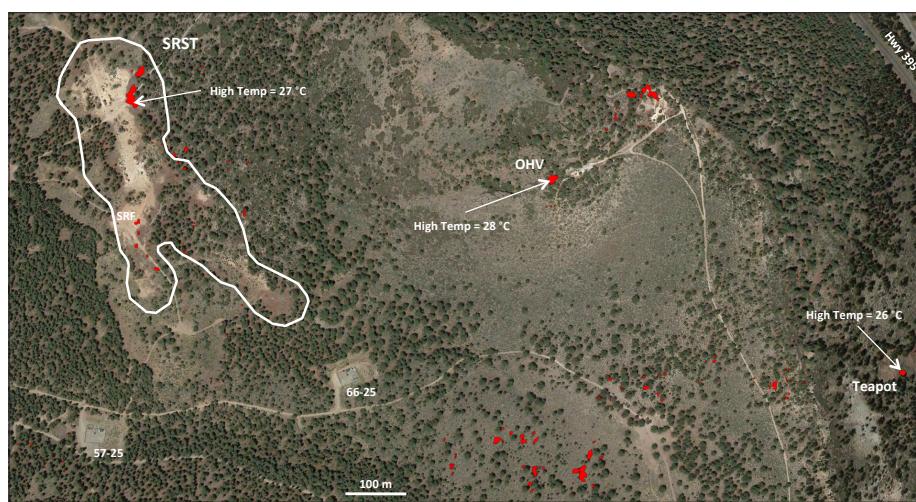


Figure 2. Google Earth image showing the SRST thermal area and the 57-25 and 66-25 production wells. The area of the flux measurement grid at SRST is outlined in white. TIR-detected hot pixels (2.3 m-pixels), which represent areas with a pre-dawn pixel temperature >16 °C, are highlighted in red. Abbreviations defined in Figure 1 caption.

Figure 3. Google Earth image showing the Sierra Star golf course at Mammoth Lakes. TIR-detected hot pixels (2.3 m-pixels), which represent areas with a pre-dawn pixel temperature of $>16^{\circ}\text{C}$, are highlighted in red. The water temperature in a pond receiving reclaimed wastewater discharge ranges up to 26°C . The pond without warm water input is thermally homogenous at $\sim 15^{\circ}\text{C}$.

warm, reclaimed wastewater discharge into a pond (Fig. 3). Water temperatures in the pond that receives warm water input range up to 26°C . The pond that receives no warm water input is thermally homogenous at $\sim 15^{\circ}\text{C}$.

Ground Temperatures and Diffuse CO_2 Emissions at SRST

Over the course of this investigation we altered the shape and size of the SRST grid in response to the formation of new areas of ground heating and associated tree kill. As of 2014 the grid includes several zones with steaming ground. As mentioned above, steaming ground near Shady Rest fumarole has been known to exist for many years, but other sites have recently been identified. In 2009 we discovered a patch of thermal ground southeast of the original grid (Fig. 4a). In subsequent years new tree kill between the SE area and the main grid prompted us to add additional sites and combine these areas (Bergfeld and Evans, 2011). The current (2014) footprint of the SRST area was established by 2011 and covers $\sim 100,000\text{ m}^2$ (Fig. 4).

Temperatures across SRST are positively correlated with diffuse CO_2 emissions (Fig. 5) with values for the coefficient of determination (r^2) between 0.30 and 0.48. Each year there are a few

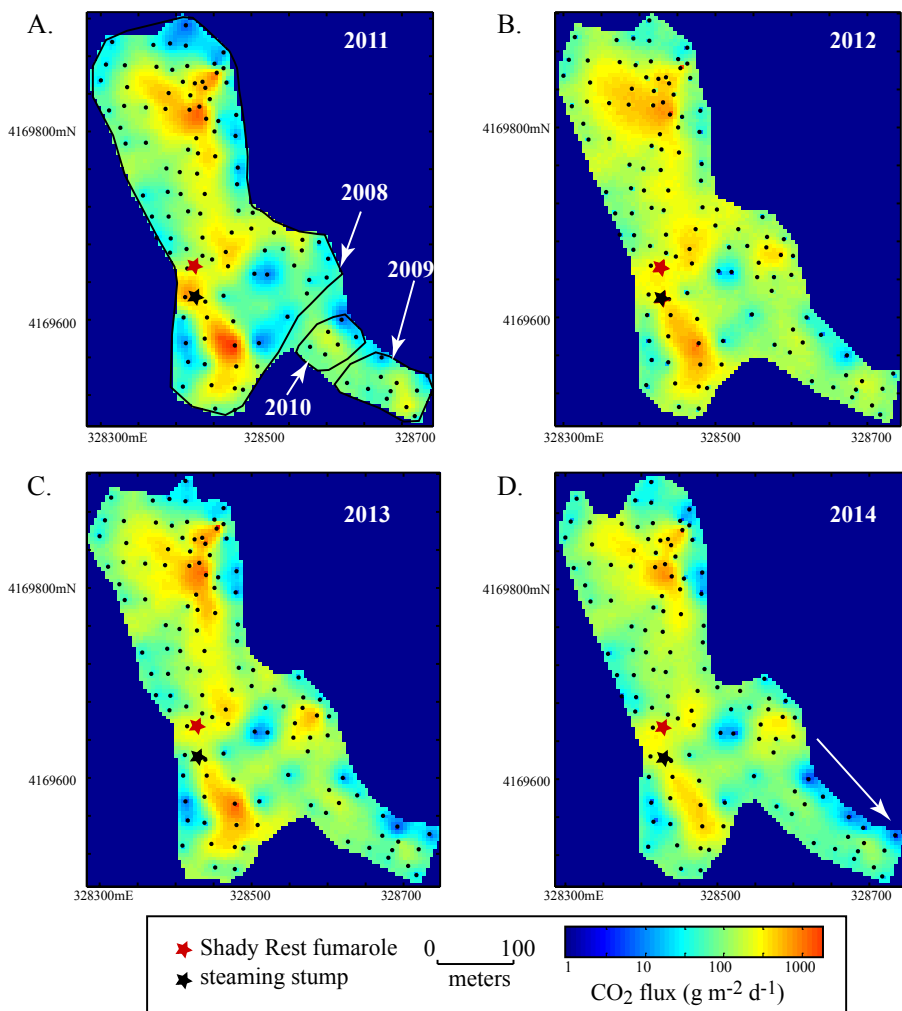
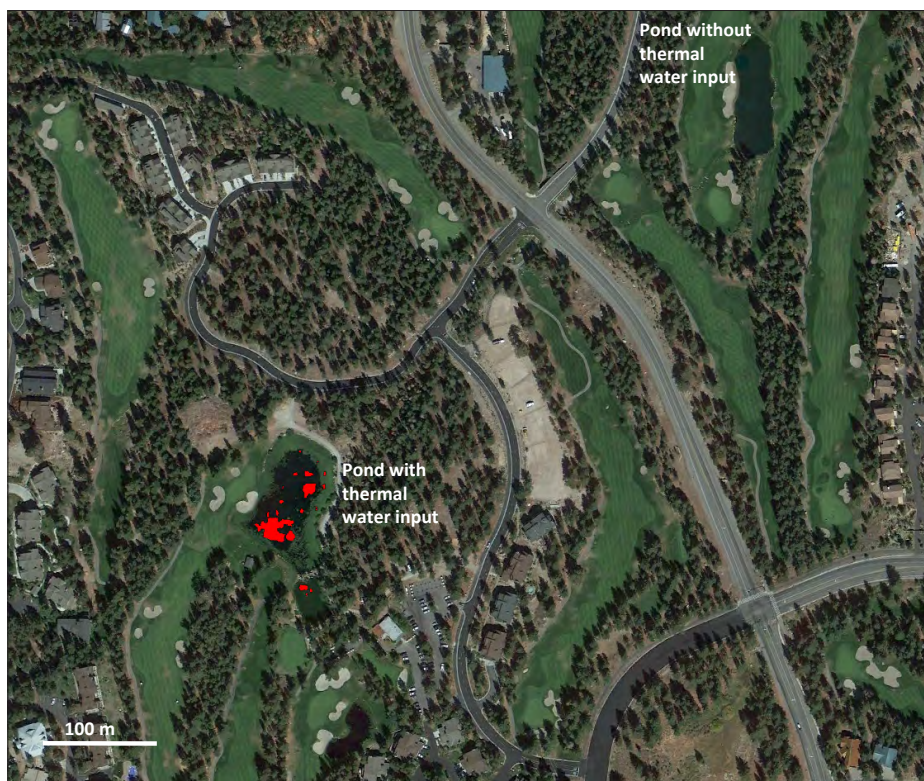


Figure 4. Contour plots from sGs calculations showing diffuse CO_2 flux at SRST in 2011 through 2014. Outlines and years listed in Figure 4A delineate measurement sites that were added to the early (2008) grid. White arrow in Figure 4D points toward the 66-25 production well.

(1–3) sites with very high flux that fall off the local flux-temperature trend. Subsurface temperatures as high as ~92 °C are found at SRF and at the base of a steaming tree stump about 65 m south of SRF, but since 2011 the maximum temperature at flux measurement grid points has been between 55–67 °C at 20 cm depth during daytime hours (Table 1). With the TIR results we can identify three main areas with elevated soil temperatures in the northeast, southwest and east-central parts of the grid (Fig. 2) that correspond with zones of high CO₂ flux in the CO₂ flux contour plots from 2011 through 2014 (Fig. 4).

Although the area of thermal ground at SRST has expanded over the past 10 years, and additional tree mortality continues to occur within the area of thermal ground, there is no trend in CO₂ emissions over the past 4 years (Fig. 4). The maximum CO₂ flux at a single site was 2800 g m⁻² d⁻¹ in 2011, but in 2012–2014 the maximum was between 1400 and 2000 g m⁻² d⁻¹ (Table 1, Fig. 5). The average flux, and therefore the total discharge, has been fairly uniform over the four years at 12–18 t d⁻¹.

Gas Compositions at SRF and Other Similar Vents

The gas composition at SRF has been monitored as far back as 1996 (Table 2). The gas consists primarily of CO₂ with an average $\delta^{13}\text{C}$ value of -3.9‰. H₂S was first detected in 2009 and has been found at generally increasing concentrations in subsequent SRF samples. Isobutane (a non-toxic gas used as the working fluid at the power plant) had not been detectable in SRF gas, but was detected at trace concentrations in 2014 using a more sensitive analytical method. Isobutane is occasionally injected into the geothermal reservoir at Casa Diablo when leaks occur in the heat exchangers, and its presence in gas emissions provides a means to track the subsurface migration of injectate from the plant (Evans and others, 2004). Isobutane was identified in gas vents closer to the power plant as early as 1995 (Evans and others, 2004; Bergfeld and Evans, 2011).

Table 2 also contains compositional and carbon isotope data from gas collected beneath the steaming stump (SS) in the SRST thermal area, gas from two samples collected from a hot

site within the Teapot thermal area and a single sample of gas collected in 2011 from the Obsidian Hill gas vent. The composition of gas collected at the steaming stump is nearly identical to SRF gas collected on the same day. The gas discharge at OHV in 2011 was weak, and the sample contains high concentrations of air-derived gas, but the $\delta^{13}\text{C}$ -CO₂ values are similar to the gas from other thermal areas. The Teapot site is located about 2 km northwest of Casa Diablo. This site was not identified in the initial survey of thermal areas (Sorey, 1998), and the first gas was collected in March 2004 (Bergfeld and Evans, 2011). The thermal ground at Teapot is characterized by the presence of cheat grass and a few

Table 1. Summary statistics of CO₂ flux and temperature data collected at SRST (2011–2014), Long Valley caldera, California. Total CO₂ discharge for each year is calculated assuming a grid area of 100,000 m².

Month-year	# of sites	Max. Soil Temp. °C	Max. flux g m ⁻² d ⁻¹	Mean flux g m ⁻² d ⁻¹	Discharge t d ⁻¹	Discharge Range t d ⁻¹
07 2011	120	67	2853	143	14.3	9-21
09 2012	123	62	1542	177	17.7	12-25
06 2013	124	65	2091	146	14.6	10-20
10 2014	122	55	1391	122	12.2	8-16

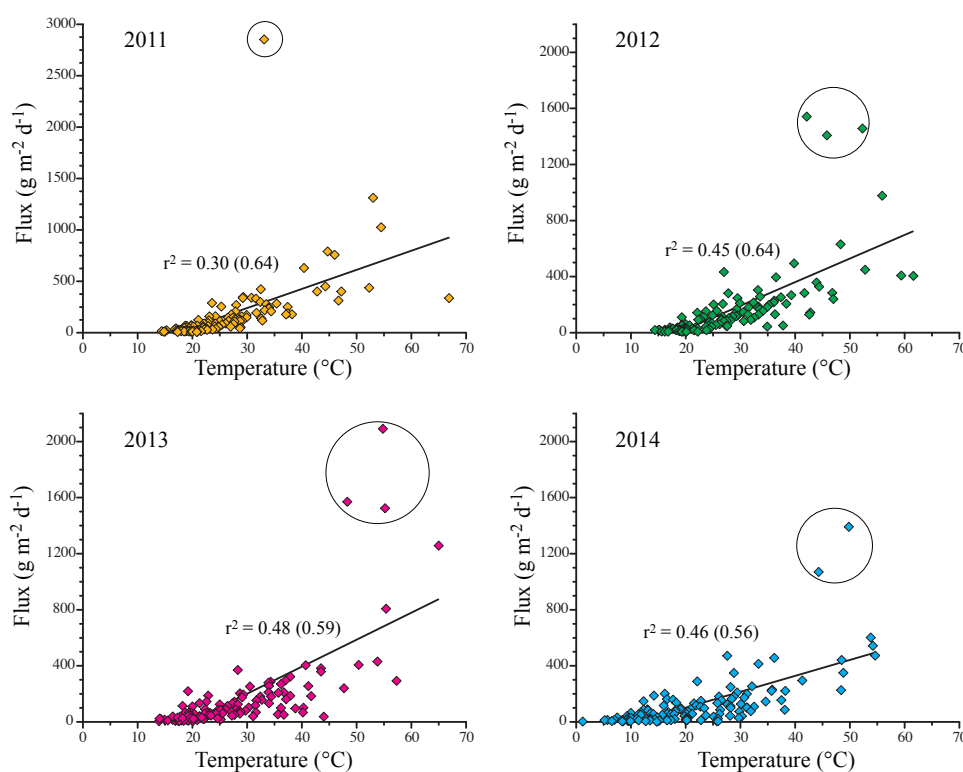


Figure 5. Scatter plots showing CO₂ flux versus soil temperature at 20 cm depth for SRST from July 2011–October 2014. Note larger scale for flux values (y-axis) in 2011. The r²-values are the coefficient of determination, calculated for linear regression of temperature and flux values. The values in parentheses are for data sets that exclude a few very high flux sites (circled).

recently killed Ponderosa Pine trees. The Teapot area lacks a discrete gas vent, and samples are collected from a site with damp soil that exhibits the maximum temperature (~93 °C at 20 cm in 2014). The gas differs slightly from SRF gas in that it contains higher concentrations of air-derived components, has somewhat lower $\delta^{13}\text{C}$ -CO₂ values, and contains higher concentrations of isobutane, consistent with its closer proximity to the Casa Diablo power plant.

Table 2. Sample locations, gas chemistry in volume percent, and permil carbon isotope values of samples collected from select thermal areas, Long Valley caldera, California. The temperature is typically measured at 30 cm, n-C₄H₁₀ and i-C₄H₁₀ are normal- and iso-butane. Hydrocarbon concentrations in bold font were determined using a gas chromatograph with a flame ionization detector. Obsidian Hills vent (OHV), Shady Rest fumarole (SRF), steaming stump (SS), not analyzed (na), not recorded (nr). ¹Data reported earlier in Bergfeld and Evans, (2011). Datum for the UTM coordinates is referenced to WGS84 zone 11.

Location	Date	Temp. (°C)	Easting (m)	Northing (m)	-----volume percent-----											$\delta^{13}\text{C}$ -CO ₂ (‰)			
					CO ₂	He	H ₂	Ar	O ₂	N ₂	CH ₄	C ₂ H ₆	H ₂ S	C ₃ H ₈	n-C ₄ H ₁₀		i-C ₄ H ₁₀		
SRF	09/25/96	90.0	328427	4169615	81.4	0.0038	0.0290	0.1588	3.0	15.0	0.0273	<0.0002	<0.0005	<0.0005	<0.0005	<0.0005	<0.0005	<0.0005	-3.9
SRF	06/19/97	nr	328427	4169615	69.1	0.0025	0.0109	0.2763	5.7	25.0	0.0232	<0.0002	<0.0005	<0.0005	<0.0005	<0.0005	<0.0005	<0.0005	na
SRF	06/06/02	89.6	328427	4169615	85.1	0.0036	0.0094	0.1302	2.7	12.0	0.0585	<0.0002	<0.0005	<0.0005	<0.0005	<0.0005	<0.0005	<0.0005	-3.7
SRF	07/14/06	91.0	328427	4169615	85.9	0.0050	0.0019	0.1322	2.4	12.0	0.0615	0.0003	<0.0005	<0.0005	<0.0005	<0.0005	<0.0005	<0.0005	-4.4
SRF	06/22/09	79.2	328427	4169615	70.9	0.0037	0.0351	0.2706	5.7	23.0	0.0489	0.0024	0.0186	<0.0005	<0.0005	<0.0005	<0.0005	<0.0005	na
SRF	09/08/10	87.9	328427	4169615	63.5	0.0022	0.0365	0.3427	7.2	29.0	0.0442	<0.0002	0.0300	<0.0005	<0.0005	<0.0005	<0.0005	<0.0005	-3.7
SRF	07/10/11	83.0	328427	4169615	94.8	0.0039	0.0299	0.0463	0.5	4.4	0.0673	<0.0002	0.0414	<0.0005	<0.0005	<0.0005	<0.0005	<0.0005	-4.0
SRF	06/21/13	88.7	328427	4169615	59.0	0.0030	0.0246	0.3878	8.2	32.3	0.0359	<0.0002	0.0007	<0.0005	<0.0005	<0.0005	<0.0005	<0.0005	na
SRF	08/23/13	nr	328427	4169615	97.8	0.0048	0.0435	0.0169	0.03	1.8	0.0672	<0.0002	0.2400	<0.0005	<0.0005	<0.0005	<0.0005	<0.0005	na
SRF	08/18/14	92.0	328427	4169615	97.9	0.0043	0.0323	0.0182	0.04	1.8	0.0722	0.0004	0.1610	0.0001	<0.0005	0.0004	<0.0005	0.0004	-3.9
SS	07/10/11	91.6	328437	4169552	97.2	0.0028	0.0095	0.0248	0.18	2.5	0.0546	<0.0002	0.0445	<0.0005	<0.0005	<0.0005	<0.0005	<0.0005	-3.9
Teapot	03/25/04	86.0	329860	4169286	73.5	0.0041	0.0565	0.2387	5.1	21.0	0.0465	<0.0002	<0.0005	<0.0005	<0.0005	<0.0005	<0.0005	0.0067	-4.4
Teapot	08/18/14	92.9	329866	4169280	89.5	0.0013	0.1565	0.0929	2.0	7.8	0.0278	0.0001	0.3933	<0.0005	<0.0005	<0.0005	0.0015	-4.3	
OHV	07/09/11	87.7	329242	4169666	60.4	0.0023	0.0002	0.3736	7.5	31.7	0.0186	<0.0002	<0.0005	<0.0005	<0.0005	<0.0005	<0.0005	<0.0005	-4.1

Monitoring Impacts of New Geothermal Development

Temperature profiles in wells near SRST (e.g. RDO-8, Fig. 1) show that vapor pressure in the thermal aquifer is near the boiling-point curve of water (Sorey and others, 1991), particularly if dissolved gases are considered. Thus, pressure drawdown related to production from wells 57-25 and 66-25 is the likely cause for the observed expansion of thermal ground (Bergfeld and Evans, 2011). Despite the uniform total CO₂ emission, the appearance of H₂S in the gas vent SRF in 2009 suggests that increased boiling at geothermal reservoir depths and/or more vigorous steam upflow could drive this soluble gas out of the water and up to the land surface. However, the higher H₂S concentrations in 2013 and 2014 could in part reflect a persistent drought and reduction in cold water availability for scrubbing the H₂S in the shallow subsurface; an eventual return to wet conditions will test this alternative hypothesis.

The presence of isobutane in SRF suggests that injectate can flow from Casa Diablo all the way to SRST, beyond the westernmost production wells, and could provide some pressure support to counterbalance fluid withdrawal from this area. The potential impact on mitigating thermal ground expansion and CO₂ emissions is difficult to estimate. Pressure support will be a key consideration as geothermal production is ramped up in this area where the thermal regime is already close to the boiling curve.

Water levels will be monitored in new wells within and around the area of expanded development, but continued tracking of ground surface temperature and CO₂ emissions could potentially reveal sites away from the wells if pressure declines occur over a broader area. The hope in combining aerial TIR imagery with existing methods is that no areas of thermal ground will go unnoticed, and that the distinction between thermal ground and background sites can be more clearly resolved. TIR can also provide annual data on thermal areas where ground-based measurements are only done sporadically, such as those near Casa Diablo.

Summary of TIR Effort

High-resolution airborne TIR data were acquired during a pre-dawn flight on October 9, 2014. Data acquisition during pre-dawn hours minimizes the effects of solar irradiance on surface temperature and maximizes the temperature contrast between the non-thermal background and thermally interesting targets.

Thermal areas ranging in size from Shady Rest to the smallest known area of thermal ground, the Teapot area, are readily identified in the images. These results provide confidence that the TIR results have captured the predevelopment

conditions, and are unlikely to have missed existing areas of thermal ground. Numerous other thermally anomalous areas were identified in the TIR imagery and will be investigated in future field work.

The TIR imagery proved useful even within an urban environment (Town of Mammoth Lakes) where numerous small heat sources such as fireplaces, automobiles, and heavy equipment were expected to cause problems. Most of these “noise” sources were filtered out at the 2.3-m pixel resolution and the 16 °C cutoff used. In fact, man-made ponds and swimming pools may offer useful calibration surfaces if instrumented with temperature loggers during future flights. The TIR imagery clearly revealed a pond that, unbeknownst to us, was receiving warm discharge water.

Our next priority is to evaluate the more detailed imagery (0.9-m pixel size) and is planned to begin in the summer of 2015, after georeferencing is finalized. Even smaller thermal anomalies are expected to be detectable in this imagery.

Acknowledgments

Jim Howle (USGS, Truckee, California) provided valuable field assistance in collecting SRST flux data for several years. Funds to collect the TIR data were provided by Collin Reinhart, Bureau of Land Management, Bishop, California. Any use of trade, firm, or product names is for descriptive purposes only and does not imply endorsement by the U.S. Government

References

- Bergfeld, D., and W.C. Evans, 2011. Monitoring CO₂ emissions in tree kill areas near the resurgent dome at Long Valley caldera, California: U.S. Geological Survey Scientific Investigations Report 2011-5038, 22 p.
- Cardellini, C., G. Chiodini, and F. Frondini, 2003. Application of stochastic simulation to CO₂ flux from soil, mapping and quantification of gas release: *J. of Geophys. Res.*, v. 108, (B9), 2425, doi:10.1029/2002JB002165.
- Coplen, T. B., 1973. A double focusing, double collecting mass spectrometer for light stable isotope ratio analysis: *Int. J. Mass Spectrom. and Ion Physics*, v. 11, p. 37-40.
- Deutsch, C.V., A.G. Journel, 1998. *GSLIB, geostatistical software library and user's guide (Applied Geostatistics Series)*, 2nd ed., Oxford University Press, 369 p.
- Evans W.C., T.D. Lorenson, M.L. Sorey, and D. Bergfeld, 2004. Transport of injected isobutane by thermal groundwater in Long Valley caldera, California, USA. In Wanty RB, Seal II RR, editors. *Water-Rock Interaction-11 2004*; p. 125-129.
- Lewicki, J.L., D. Bergfeld, C. Cardellini, G. Chiodini, D. Granieri, N. Varley, and C. Werner, 2005. Comparative soil CO₂ flux measurements and geostatistical estimation methods on Masaya volcano, Nicaragua: *Bull. Volcanol.*, v. 68, no. 1, p. 76-90.
- Révész, K., and Coplen, T.B., eds., 2006. *Methods of the Reston Stable Isotope Laboratory: U.S. Geological Survey Techniques and Methods*, book 10, chap. C20, 38 p.
- Sorey, M.L., G.A. Suemnicht, N.C. Sturchio, and G.A. Nordquist, 1991. New evidence on the hydrothermal system in Long Valley caldera, California, from wells, fluid sampling, electrical geophysics, and age determinations of hot-spring deposits. *J. Volcanol. Geotherm. Res.*, 48, 229–263.
- Sorey, M.L., C.D. Farrar, G.A. Marshall, and J.F. Howle, 1995. Effects of geothermal development on deformation in the Long Valley caldera, eastern, California. *J. Geophys. Res.* 100, B7, 12475-12486.
- Sorey, M.L., W.C. Evans, B.M. Kennedy, C.D. Farrar, L.J. Hainsworth, and B. Hausback, 1998. Carbon dioxide and helium emissions from a reservoir of magmatic gas beneath Mammoth Mountain, California *J. Geophys. Res.*, 103, B7, 15,303-15,323.
- Suemnicht, G.A., M.L. Sorey, J.N. Moore, and R. Sullivan, 2007. The shallow hydrothermal system of Long Valley caldera, California. In: *Proceedings. Stanford, California, Thirty-Second Workshop on Geothermal Reservoir Engineering; 01/22/2007; Stanford, California*. San Diego, CA: Stanford University; p. 465-470.

